Biotechnology Reports 46 (2025) e00889

Contents lists available at ScienceDirect

Biotechnology Reports

journal homepage: www.elsevier.com/locate/btre

Optimized expression of human interleukin-15 in *Nicotiana benthamiana* and *in vitro* assessment of its activity on human keratinocytes

Chalatorn Charnsatabut [a,b], Pipob Suwanchaikasem [c], Kaewta Rattanapisit [c], Iksen Iksen [d], Varisa Pongrakhananon [e,f], Christine Joy I. Bulaon [c,*], Waranyoo Phoolcharoen [a,b,*]

[a] Center of Excellence in Plant-produced Pharmaceuticals, Chulalongkorn University, Bangkok 10330, Thailand
[b] Department of Pharmacognosy and Pharmaceutical Botany, Faculty of Pharmaceutical Sciences, Chulalongkorn University, Bangkok 10330, Thailand
[c] Baiya Phytopharm Co., Ltd., Bangkok 10330, Thailand
[d] Department of Research and development, Provenedge Co. Ltd., Bangkok 10330, Thailand
[e] Department of Pharmacology and Physiology, Faculty of Pharmaceutical Sciences, Chulalongkorn University, Bangkok 10330, Thailand
[f] Center of Excellence in Preclinical Toxicity and Efficacy Assessment of Medicines and Chemicals, Chulalongkorn University, Bangkok 10330, Thailand

ARTICLE INFO

Keywords:
Nicotiana benthamiana
Human interleukin-15
Cytokine
Cell proliferation
Wound healing

ABSTRACT

Human interleukin-15 (hIL-15) is a cytokine essential for immune modulation with therapeutic applications in cancer and chronic wound healing. Although hIL-15 is commercially available, large-scale production studies remain limited. With promising clinical trial results, demand for hIL-15 is expected to rise. Plant expression systems offer a sustainable, low-cost alternative for rapid biopharmaceutical production. In this study, we optimized hIL-15 expression in *Nicotiana benthamiana* and assessed its physicochemical properties and biological activity. We fused hIL-15 to the Fc domain of human IgG1 for efficient purification. Through optimization of the pre- and post-infiltration conditions, we achieved transient expression and recovery at 4 dpi, yielding 33.8 μg/g fresh weight. Peptide mapping confirmed 97 % overall sequence coverage of the primary structure. Treatment with plant-produced hIL-15-Fc effectively promoted human keratinocyte HaCaT cell proliferation and migration *in vitro*. These findings demonstrated the potential of plant-based platforms for producing therapeutic recombinant hIL-15 that support wound healing.

1. Background

Human interleukin-l5 (hIL-15) is a 14–15 kDa glycoprotein first reported as a T cell proliferation factor or T cell growth factor in 1994 [1]. This cytokine belongs to the same group as IL-2 and share similar functions, including the stimulation of T cell proliferation, the generation of cytotoxic effector T cells, immunoglobulin production by B-cells, and activation and prolonged survival of NK cells [2,3]. Both cytokines signal through shared heterodimeric receptors, specifically the IL-2/15 Rβ and the γc subunit. Furthermore, hIL-15 plays a role in chronic wound healing by promoting the proliferation of HaCaT keratinocytes via the AKT and ERK1–2 pathways, as well as facilitating tissue regeneration in liver damage [4,5].

The hIL-15 is commercially available; however, there are few studies focused on the up-scaling of its production. Previous research attempted to produce hIL-15 in various systems, including yeast, bacteria, and mammalian cells [6–8]. Clinical trials have investigated the use of recombinant *Escherichia coli*-derived hIL-15 in combination with monoclonal antibodies Nivolumab and Ipilimumab [9]. The first trial reported the successful elimination of circulating adult T cell leukemia and chronic lymphocytic leukemia in select patients. As evidence of its therapeutic potential continues to grow, hIL-15 is predicted to play an increasingly prominent role in cancer treatment, particularly when combined with anti-tumor drugs to enhance efficacy [10].

In the present study, we focused on producing hIL-15 in *Nicotiana benthamiana* as part of an effort to identify scalable and cost-effective production platforms. Several expression platforms are available for the production of therapeutic recombinant proteins, each with distinct advantages regarding yield, post-translational modifications (PTMs), growth rate, cost, and safety [11]. Plant-based expression systems have been widely used due to their ability to produce high-value recombinant proteins comparable to mammalian cells [12]. Key benefits of these platforms include rapid growth, the capacity for complex PTMs, low operational costs, ease of optimization, and scalability [11–16]. Among

* Corresponding authors.
E-mail addresses: christine.b@baiyaphytopharm.com (C.J.I. Bulaon), Waranyoo.p@chula.ac.th (W. Phoolcharoen).

https://doi.org/10.1016/j.btre.2025.e00889
Received 30 October 2024; Received in revised form 16 January 2025; Accepted 25 March 2025
Available online 25 March 2025

the *Nicotiana* species, *N. benthamiana*, a tobacco plant native to Australia, is especially notable for its high susceptibility to a wide range of plant pathogens [12,17] and its suitability for transient protein expression through *Agrobacterium*-mediated transformation [18].

Fc fusion proteins, which link the Fc domain of human immunoglobulin G (IgG) to a target protein, offer several advantages for therapeutic use. The Fc fragment increases the molecular size of the protein, prolonging its half-life by reducing clearance. Additionally, Fc fusion enables FcRn-mediated recycling, wherein the Fc region binds to FcRn at acidic pH, preventing degradation. The complex is then released back into the circulation at neutral pH, effectively extending its presence in the system [19–22]. The Fc domain also enhances the solubility and stability of the fusion target by independent folding and structural support [23]. Moreover, Fc fusion proteins can be easily purified via Protein A affinity chromatography [24]. The safety and efficacy of Fc fusion proteins have been well-established in clinical trials. For example, the fusion of the tumor necrosis factor receptor (TNFR) with Fc has proven effective in treating rheumatoid arthritis, reducing disease activity without dose-limiting toxicity, significant hematologic abnormalities, or immunogenic responses to TNFR-Fc [25]. Additionally, APG101, a glycosylated CD95 receptor fused with Fc, was administered to healthy volunteers and two patients with malignant glioma without eliciting side effects and anti-drug antibodies. These findings further indicate the safety of Fc fusion proteins [26]. Previous studies have successfully tagged Fc to a variety of proteins, which includes toxins, receptors, ligands, drugs, and some cytokines like IL-2, IL-4, and TNF [27–29].

In this study, we implemented various strategies to optimize hIL-15-Fc expression in *N. benthamiana,* including the use of different expression cassettes and agrotransformation conditions. The hIL-15-Fc fusion protein was transiently expressed, characterized, and tested *in vitro* for its biological activity on HaCaT cell proliferation and migration.

2. Materials and methodology

2.1. Expression vector construction

The amino acid sequence of hIL-15 was obtained from the UniProt database (Entry P40933–1) and optimized *in silico* for expression in *N. benthamiana* (GeneArt gene synthesis, Thermo Fisher Scientific). Three constructs of hIL-15 were designed as shown in Fig 1. The Fc domain of IgG1 was fused to the C-terminus of hIL-15 to form the "hIL-15-Fc" cassette. Additionally, the "SP-hIL-15-Fc" and "SP-hIL-15-Fc-KD" constructs included a signal peptide (SP) at the N-terminus and with the latter incorporating the SEKDEL (KD) sequence at the C-terminus. Each expression cassette contained *Xba*I and *Sac*I restriction sites to facilitate cloning of hIL-15 into the pBYR2eK expression vector [30]. The recombinant vector was transformed into *E. coli* DH10B by heat shock method and grown on LB plates containing 50 μg/mL kanamycin. Resulting colonies were screened by PCR to confirm the presence of the correct recombinant clones.

2.2. Evaluation of different hIL-15-Fc expression cassettes for efficient expression

The hIL-15 expression vectors were transformed into *Agrobacterium tumefaciens* GV3101 by electroporation. Transformed cells were cultivated on LB agar plates supplemented with 50 μg/mL of kanamycin, rifampicin, and gentamicin for 48 h at 28 °C. Successful transformation of *A. tumefaciens* clones was confirmed by PCR. Positive colonies were then inoculated into antibiotic-selective LB broth with constant shaking (200 rpm) at 28 °C. Overnight-grown *Agrobacterium* cells were centrifuged at 6,000 rpm for 5 min. For transient infiltration, cell pellets were resuspended in 1X infiltrate buffer (10 mM 2-N-morpholino-ethanesulfonic acid; MES and 10 mM $MgSO_4$) to obtain a final OD_{600} of 0.2. Approximately 4-week-old *N. benthamiana* leaves were infiltrated using a syringe without needle and left for 4 days.

To identify the expression level of each hIL-15 construct, infiltrated plant leaves were collected and extracted with PBS buffer pH 7.4. Crude extracts were centrifuged at 13,000 rpm for 10 min to discard cell debris. Protein samples were analyzed by SDS-PAGE and Western blot.

2.3. Optimization of agroinfiltration in plants

To evaluate the effect of plant age on hIL-15-Fc expression, *Agrobacterium tumefaciens* cultures were resuspended to an OD_{600} of 0.2 and infiltrated into 3-, 4-, and 5-week-old tobacco plants. Leaf samples were collected at 4 dpi. For optimization of *Agrobacterium* cell density, bacteria cultures were pelleted and resuspended to final OD_{600} values of 0.1, 0.2, 0.4, and 0.8. Each concentration was infiltrated into different regions of the same *N. benthamiana* leaf. Leaf samples were collected at 4 dpi and then extracted. To optimize the harvesting time, *Agrobacterium* cultures at an OD_{600} of 0.2 were infiltrated into *N. benthamiana* plants. Leaf samples were collected at 2, 4, 6, 8, and 10 dpi and extracted with

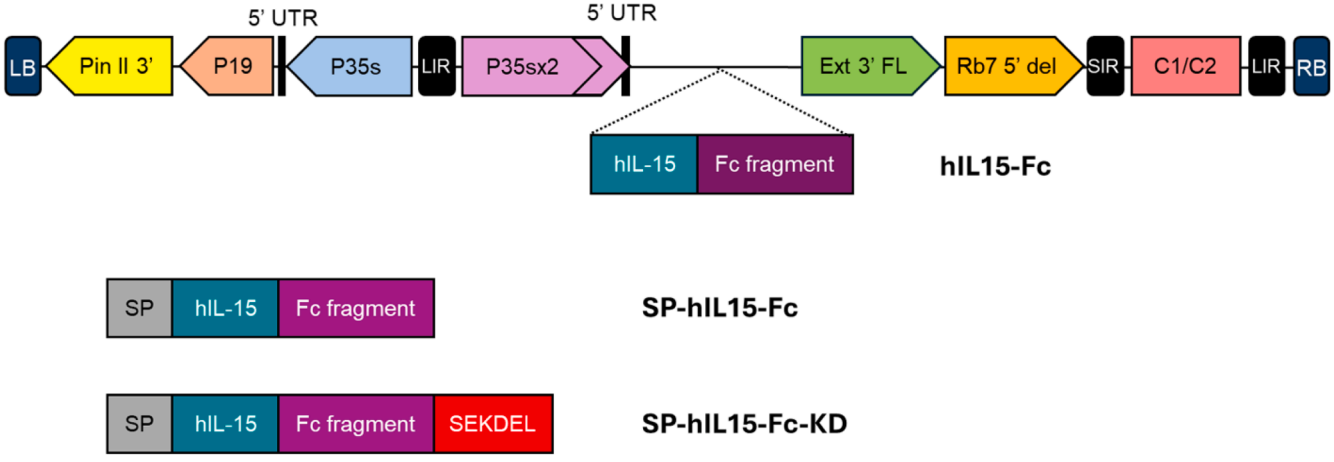

Fig. 1. Schematic representation of different pBYR2eK-hIL-15-Fc expression cassettes based on subcellular targets in plant cells; LB and RB: the left and right margins of T-DNA; Pin II 3′: the potato proteinase inhibitor II gene; P19: P19 gene from Tomato Bushy Stunt Virus (TBSV); P35s: Cauliflower Mosaic Virus (CaMV) 35 s promoter; P35sx2: CaMV 35 s promoter with duplicated enhancer; Ext 3′ FL: tobacco extension gene; Rb7 5′ del: tobacco Rb7 promotor; C1/C2: Bean Yellow Dwarf Virus (BeYDV) ORFs C1 and C2 encoding replication initiation protein (Rep) and RepA protein; LIR: long intergenic region of BeYDV; SIR: short intergenic region of BeYDV; hIL15-Fc: hIL-15 gene with Fc fragment at the C-terminus; SP-hIL15-Fc: hIL-15 gene with signal peptide at the N-terminus and Fc fragment at the C-terminus; SP-hIL15-Fc-KD: hIL-15 gene with signal peptide at the N-terminus and Fc fragment and SEKDEL ER retention sequence at the C-terminus.

PBS buffer pH 7.4.

Protein expression levels from each optimization experiment were analyzed by Western blotting under non-reducing conditions. Membranes were probed with rabbit anti-hIL-15 followed by HRP-conjugated goat anti-rabbit antibody. Band intensities from the blots were used to quantify hIL-15-Fc expression.

2.4. Plant-produced hIL-15-Fc purification

For purification, vacuum-mediated agroinfiltration was used for the transient transformation of *N. benthamiana* plants. About 50 g of infiltrated leaves were harvested at 6 dpi and homogenized with cold PBS buffer pH 7.4 at a 1:2 ratio using a blender. The homogenate was centrifuged at 13,000 rpm for 1 h, and the resulting supernatant was further clarified using a 0.45 μm membrane filter (Merck, USA).

The filtered crude lysate was loaded onto a column packed with MabSelect SuRe™ Protein A affinity resin (Cytiva, USA), equilibrated with PBS buffer pH 7.4. The recombinant hIL-15-Fc was eluted with 0.1 M glycine pH 2.7 and immediately neutralized with 1.5 M Tris–HCl pH 8.8 to obtain a final pH of 7.

2.5. SDS-PAGE and Western blot analysis

A total of 10 μg total soluble protein and 3 μg purified hIL-15-Fc were mixed with 6x reducing loading dye (125 mM Tris–HCl pH 6.8, 12 % w/v SDS, 10 % v/v glycerol, 22 % v/v β-mercaptoethanol, and 0.001 % w/v bromophenol blue) or 6x non-reducing loading dye (125 mM Tris–HCl pH 6.8, 12 % w/v SDS, 10 % v/v glycerol, and 0.001 % w/v bromophenol blue). The samples were then loaded onto a 10 % polyacrylamide gel and stained with One-Step Blue® Protein dye (Biotium, USA). For Western blotting, the separated proteins were transferred to nitrocellulose membrane (Bio-Rad, USA) and blocked with 5 % w/v skim milk in PBS buffer pH 7.4. The recombinant hIL-15-Fc was detected using rabbit anti-IL-15 (PeproTech, USA) as the primary antibody and HRP-conjugated goat anti-rabbit (Abcam, UK) as the secondary antibody, diluted 1:5,000 in 3 % w/v skim milk. Chemiluminescence detection was performed using ECL plus detection reagent (GE Healthcare, UK).

2.6. Characterization of plant-produced hIL-15 by peptide mapping analysis

Plant-produced hIL-15-Fc was buffer-exchanged and desalted using a 6,000 Da MWCO desalting column with 50 mM ammonium bicarbonate. Approximately 10 μL of at least 0.5 mg/mL purified protein was treated with 100 mM dithiothreitol for 30 min at 65 °C, followed by iodoacetamide for 20 min at 25 °C in the dark. The protein sample was then digested with 0.5 μg of trypsin and incubated for 4 h. Digested peptides were analyzed using an Agilent model 6545XT AdvanceBio LC/Q-TOF system with a Dual Agilent Jet Stream Electrospray Ionization (Dual AJS ESI) source. Separation was achieved on an Agilent AdvanceBio Peptide Mapping Column (2.1 × 150 mm, 2.7 μm). Data analysis was performed using Agilent MassHunter BioConfirm Software version 11.0.

2.7. Cell culture

Human keratinocyte HaCaT cells (ATCC, USA) were cultured in DMEM medium supplemented with 10 % fetal bovine serum, 100 U/mL penicillin-streptomycin, and 2 mM L-glutamine. The cells were maintained in a humidified incubator at 37 °C with 5 % CO_2. All media and supplements were procured from Gibco, USA.

2.8. Cell proliferation assay

HaCaT cells were seeded onto a 96-well culture plate at a density of 2,000 cells/well and incubated overnight. The cells were then treated with varying concentrations (from 1 to 20 ng/mL) of either plant-produced hIL-15-Fc or Fc for 72 h. Cell proliferation was assessed by an addition of 3-(4,5-dimethylthiazol-2-yl)-2,5-diphenyltetrazolium bromide (MTT) solution (0.5 mg/mL), following incubation for 4 h. The resulting formazan product was solubilized using DMSO, and optical density was measured at 570 nm using a microplate reader (VICTOR3/Wallac 1420, Perkin Elmer, USA). The percentage of cell proliferation was calculated relative to non-treated control cells.

2.9. Scratch wound assay

HaCaT cells were seeded onto a 24-well culture plate at a density of 130,000 cells/well overnight. Wounds were created by scraping the cell monolayer with a pipette tip, and detached cells were washed with PBS buffer pH 7.4 twice. The cells were then treated with either plant-produced hIL-15-Fc or Fc from 0–10 ng/mL. Wound areas were photographed at 0 and 24 h. The wound area was quantified using Fiji ImageJ software and expressed as a relative value to the initial wound area at 0 h.

2.10. Statistical analysis

Data are expressed as the mean ± standard deviation (mean ± SD) derived from at least three independent experiments. Statistical analysis was performed using GraphPad Prism 9 (GraphPad Software, USA). One-way analysis of variance (ANOVA), followed by Tukey's or Dunnett's multiple comparison test, was used to assess statistical significance. P-value < 0.05 was considered significant.

3. Result

3.1. Determination of optimal hIL-15-Fc expression vector

The codon-optimized nucleotide sequence of hIL-15 was fused to the Fc domain of IgG1 and cloned into the geminiviral expression vector pBYR2eK, generating three different constructs (Fig 1). To assess protein expression levels, *N. benthamiana* leaves were infiltrated with *A. tumefaciens* carrying each hIL-15 expression cassette. After 4 days, necrosis was observed on the injected leaf, with "SP-hIL15-Fc-KD" showing the most evident necrotic symptoms (Fig 2A). Nonetheless, crude extract from this construct exhibited the highest expression level of recombinant hIL-15-Fc, as confirmed by Western blot analysis and ImageJ measurement (Fig 2B, Supplementary Fig S1, and Supplementary Table S1). Necrosis may suggest cytotoxicity or plant stress due to overexpression, which requires further investigation. The strongest band intensity around 50 kDa was detected for "SP-hIL-15-Fc-KD", with a value of 53,000. The "SP-hIL-15-Fc" construct showed a lower band intensity of 35,000, while no detectable signal was observed for the "hIL-15-Fc" construct. Based on these findings, the SP-hIL-15-Fc-KD construct was selected for the next experiments.

3.2. Optimization of hIL-15-Fc expression

To optimize hIL-15-Fc expression in *N. benthamiana,* various pre- and post-agroinfiltration parameters were evaluated, including plant age, *Agrobacterium* concentration (OD_{600}), and harvest time post-infiltration (dpi).

In terms of plant age, infiltrated *N. benthamiana* leaves were harvested at 4 dpi. Western blot analysis revealed that the highest expression level was achieved in 3-week-old plants and reduced expression levels in 4- and 5-week-old plants (Fig 3A and Supplementary Fig S2). However, no statistically significant differences in hIL-15-Fc expression were detected across the different ages ($p > 0.05$) (Supplementary Table S2). Therefore, 3-week-old tobacco plants were selected for further experiments due to their slightly higher expression.

The influence of *Agrobacterium* cell culture density on hIL-15-Fc expression was examined at OD_{600} values of 0.1, 0.2, 0.4, and 0.8. The

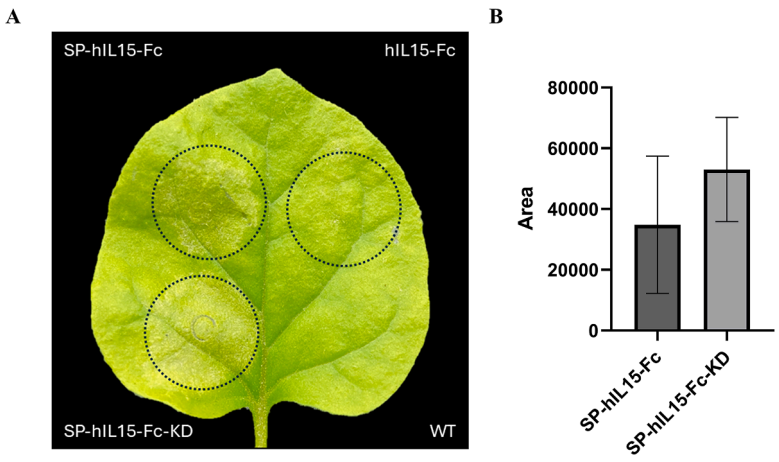

Fig. 2. Expression of three different recombinant hIL-15-Fc cassettes. Necrosis observed in *N. benthamiana* leaves at 4 dpi (A). Western blot of plant-produced hIL-15-Fc from crude extracts under reducing condition (B). Expression level from SP-hIl-15-Fc and SP-hIL15-Fc-KD. Proteins were transferred to a nitrocellulose membrane and probed with rabbit anti-hIL15 and HRP-conjugated goat anti-rabbit antibodies. Equal amounts of total soluble protein were loaded in each lane.

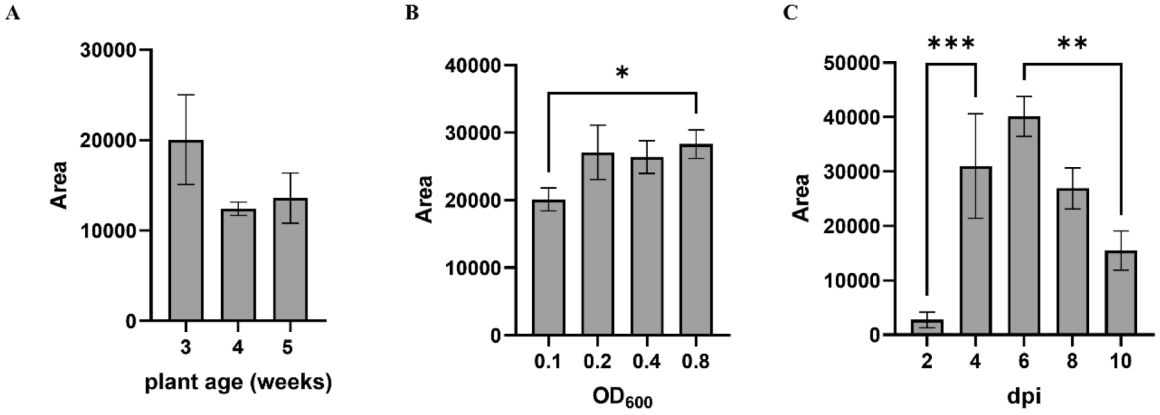

Fig. 3. Expression levels of plant-produced hIL15-Fc following optimization of *N. benthamiana* age (A), *Agrobacterium* cell density (OD_{600}) for infiltration (B), and harvest time after infiltration (dpi) (C). Expression was assessed by band intensities from Western blot analysis, probed with rabbit anti-IL15 and HRP-conjugated goat anti-rabbit antibodies. Data are presented as mean ± SD from three independent experiments. (* $p < 0.05$; ** $p < 0.01$; *** $p < 0.001$).

highest expression level was observed at OD_{600} of 0.2, though no significant differences were found between OD_{600} values of 0.2, 0.4, and 0.8 (Fig 3B and Supplementary Fig S3). However, expression at OD_{600} 0.1 was significantly lower than at OD_{600} 0.8 ($p < 0.05$) (Supplementary Table S3). Based on these results, an OD_{600} of 0.2 was chosen due to its sufficient expression levels and lower cell density for practical large-scale infiltration.

Post-infiltration harvest time was evaluated by collecting leaves at 2, 4, 6, 8, and 10 dpi. Recombinant protein expression increased significantly from 2 to 4 dpi ($p < 0.05$), reaching a peak at 6 dpi (Fig 3C and Supplementary Fig S4). Nonetheless, there was no significant difference in expression levels between 4 and 6 dpi ($p > 0.05$) (Supplementary Table S4). After 6 dpi, hIL-15-Fc expression gradually decreased at 8 and 10 dpi.

Based on these optimizations, the optimal conditions for hIL-15-Fc expression were determined to be: 3-week-old *N. benthamiana,* an *Agrobacterium* OD_{600} of 0.2, and a harvest time of 6 dpi.

3.3. Purification and size-exclusion chromatography of plant-produced hIL-15-Fc

The plant-expressed hIL-15-Fc was purified from the clarified crude extract using Protein A affinity chromatography. To confirm the size and characteristics of the purified hIL-15-Fc, the protein was analyzed by SDS-PAGE and immunoblotting under both reduced and non-reduced

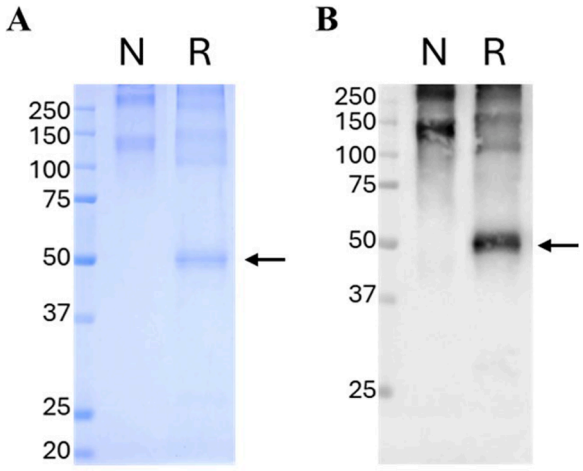

Fig. 4. The SDS-PAGE and Western blot of purified hIL-15-Fc produced in *N. benthamiana*. Infiltrated leaves were collected, and the hIL-15-Fc was purified using affinity chromatography. The purified protein was analyzed by SDS-PAGE (A) and Western blot probed with rabbit anti-IL15 and HRP-conjugated goat anti-rabbit antibodies (B). NR: purified hIL-15-Fc under non-reducing condition, R: purified hIL-15 under reducing condition.

conditions (Fig 4 and Supplementary Fig S5). The predicted molecular weight of hIL-15-Fc was 42 kDa in its monomeric form and 84 kDa in its dimeric form. However, SDS-PAGE and western blot results revealed two major bands at approximately 140 and >250 kDa under non-reducing condition, both of which were higher than the expected sizes. Under reducing condition, one major band at approximately 50 kDa was observed, which is slightly larger than the predicted molecular weight of the monomer. Trace amounts of proteins at 100, 150, and >250 kDa were also observed under reduced condition. The yield of purified hIL-15-Fc was approximately 33.8 μg per gram of fresh weight.

3.4. Characterization of plant-produced hIl-15-Fc using peptide mapping analysis

Peptide mapping of plant-produced hIL-15-Fc was performed to confirm the protein's identity and sequence. A total of 2,175 peptides were identified, with 269 matching the amino acid sequences of both the active form of hIL-15 and the immunoglobulin heavy constant gamma 1. Mass spectrometric analysis using a protein database search showed a 96.5 % sequence coverage of the hIL-15 molecule and 100 % coverage of Fc domain of IgG1 for plant-produced hIL-15-Fc, in total of 97 % overall sequence coverage. This high level of coverage indicated that majority of the protein sequence was correct and aligned with the expected amino acid sequence [31] (Fig 5 and Supplementary Fig S6).

3.5. Plant-produced hIL-15-Fc enhances keratinocyte proliferation and wound healing

In the HaCaT cell proliferation assay, treatment with plant-produced hIL-15-Fc at 1 ng/mL significantly enhanced keratinocyte proliferation, resulting in approximately 120 % cell growth (Fig 6A and Supplementary Table S5) ($p < 0.05$). This effect further increased to 140 % at 20 ng/mL. However, no significant differences in proliferation were observed between 1, 5, 10, and 20 ng/mL concentrations, indicating similar effects at higher doses ($p > 0.05$). Conversely, Fc protein alone did not exhibit any significant impact on HaCaT cell growth. These findings demonstrate the potent proliferative activity of plant-produced hIL-15-Fc.

In the scratch wound healing assay, plant-produced hIL-15-Fc significantly promoted keratinocyte migration, reducing the wound area in a dose-dependent manner (Fig 6B and 6D) ($p < 0.05$). The relative wound area was reduced to approximately 0.45, 0.4, and 0.25-fold in cells treated with 1, 5, and 10 ng/mL of hIL-15-Fc, respectively, compared to 0.71-fold in non-treated control cells after 24 h (Supplementary Table S6). On the contrary, Fc treatment did not affect cell migration at any tested concentrations (Fig 6C and 6E). These findings highlight the significant wound healing effect of plant-produced hIL-15-Fc on keratinocytes.

4. Discussion

Plant molecular farming is a biotechnology approach that uses plants as production systems for producing valuable recombinant proteins. This method utilizes the natural biological processes of plants to produce biopharmaceuticals, vaccines, enzymes, antibodies, cytokines, and other therapeutic proteins [32,33]. Compared to traditional production systems, such as bacteria, yeast, or mammalian cells, plant-based platforms offer a cost-effective and scalable alternative for recombinant protein production.

Plants have been successfully used to produce several recombinant cytokines, which are essential for disease treatment, immune function research, cell culture experiments, and improving vaccine efficacy [34, 35]. The production of multiple cytokines and growth factors across different plant species further highlights the potential of plant molecular farming in biopharmaceutical manufacturing. For instance, TNFα was produced in potatoes, obtaining 15 μg per gram of plant tissue, while IL-18 was expressed in tobacco plants with yields reaching up to 0.05 % of the total soluble protein [34]. Granulocyte-macrophage colony-stimulating factor was produced in *N. benthamiana* via a viral vector, with yields of up to 2 % total soluble protein [35]. IL-37b and IL-38 were produced in tobacco, reaching yields of approximately 1 g per kg of fresh leaf biomass [36].

Plant expression systems offer several advantages for the production of recombinant therapeutic proteins; however, certain limitations must be addressed to optimize their efficiency and ensure the safety of plant-derived therapeutics. One critical limitation is the difference in

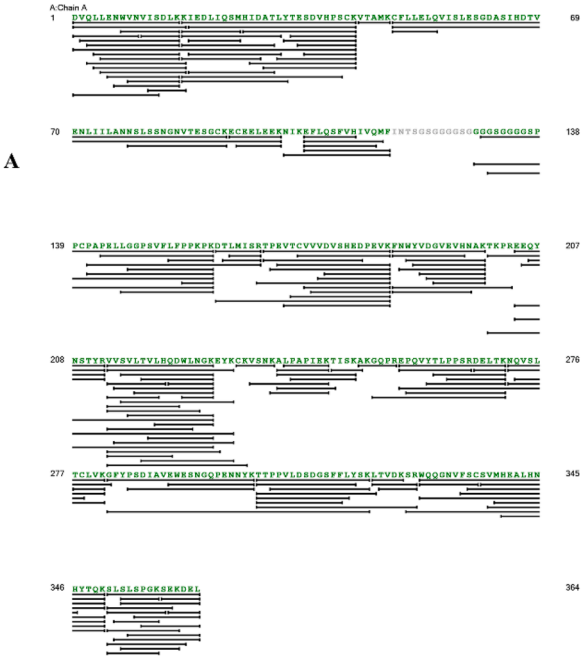

A

B

Molecule	Sequence coverage (%)
hIL-15	96.5
Fc domain of IgG 1	100

Fig. 5. Peptide mapping analysis using LC/Q-TOF (A) and sequence coverage of generated peptide compared to the hIL-15 and Fc domain of IgG1 (B). Peptide mapping generated 2,175 short peptides and 269 of them matched with the primary structure of plant-produced hIL-15-Fc.

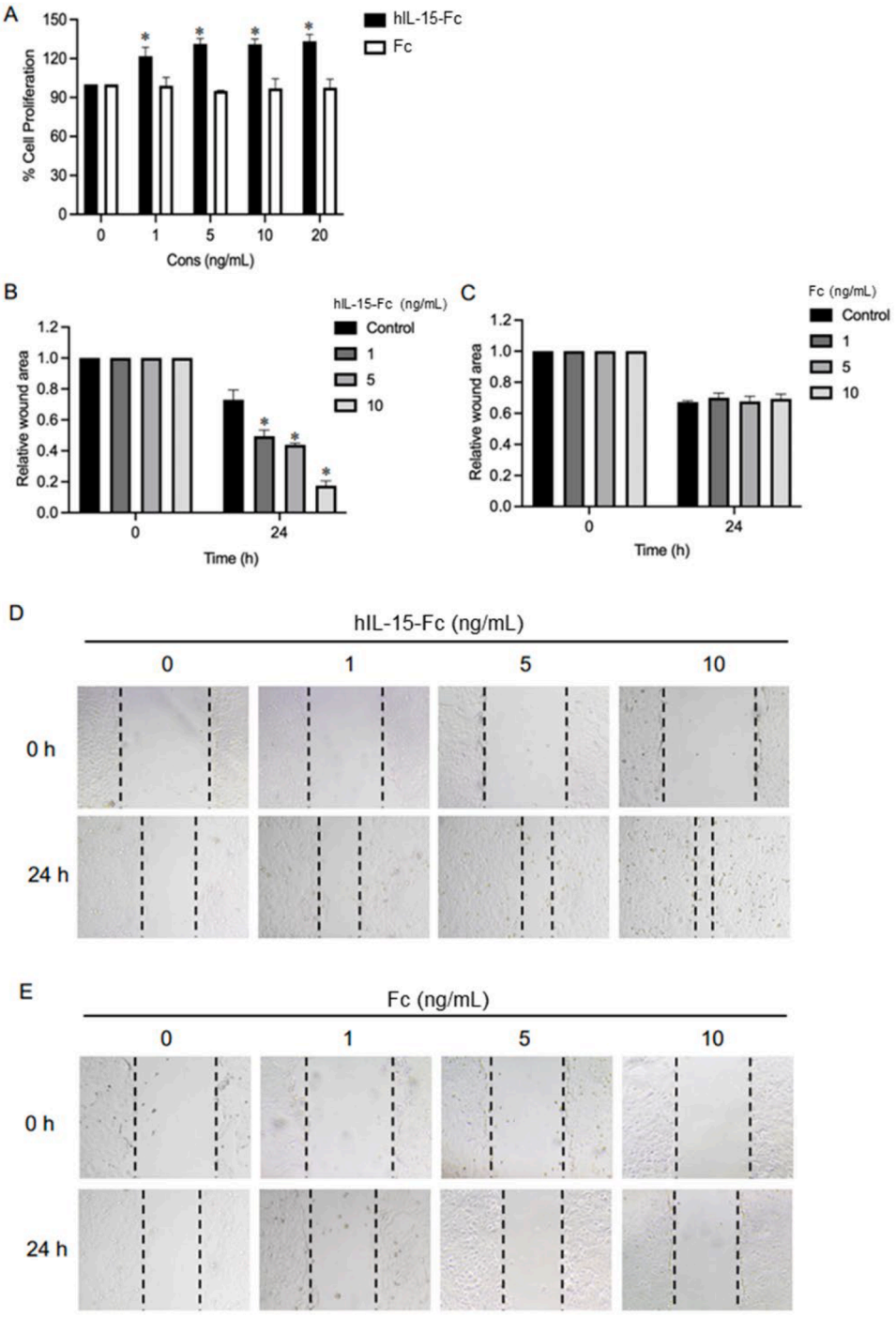

Fig. 6. The effect of plant-produced hIL-15-Fc on keratinocyte proliferation and migration. HaCaT cells were treated with hIL-15-Fc (0–20 ng/mL) for 72 h, and cell proliferation was evaluated using the MTT assay (A). The plot represents the percentage of cell proliferation relative to the non-treated control group. Data are presented as mean ± SEM ($n = 3$). *$p < 0.05$ vs. non-treated control cells. HaCaT cells were treated with either hIL-15-Fc (B) or Fc fragment (C) at 1, 5, and 10 ng/mL concentrations for 24 h, and cell migration was determined using the wound scratching assay. Wound areas in hIL-15-Fc (D) and Fc fragment (E) groups were quantified at each concentration at 24 h and normalized to the initial wound area at 0 h. Data are presented as mean ± SEM ($n = 3$). *$p < 0.05$ vs. non-treated control cells.

glycosylation patterns between plants and mammalian systems. Plant-derived glycans, such as complex-type N-glycan with β1,2-xylose and core α1,3-fucose (GnGnXF) differ structurally from mammalian glycans and have been reported to induce immunogenicity in mammalians [37, 38]. For example, McManus et al. demonstrated that administration of plant enzymes and lectins containing plant-specific glycans in laboratory rats led to the production of rat anti-xylose and fucose monoclonal antibodies [37]. These findings highlight the need for careful consideration of glycan structures in therapeutic proteins. Other PTMs, such as phosphorylation and ubiquitination, also affect recombinant protein functionality. Phosphorylation is vital for modulating protein activity, stability, and interactions [39,40]. Ubiquitination, on the other hand, primarily regulates protein degradation pathways and cellular localization in plants [40]. Future studies should further explore these modifications to maximize their potential benefits while minimizing any adverse impacts on protein production.

In this study, the immunoglobulin Fc region was fused to recombinant IL-15. The Fc region contains a single conserved N-linked glycosylation site at Asn297 within the CH2 domain, which is crucial for its structural integrity and biological activity. As mentioned above, non-human glycosylation patterns in plant-produced recombinant proteins, including Fc fusion proteins, can trigger undesirable immune responses. Stability is another significant concern, as Fc fusion proteins produced in plants often exhibit reduced stability, resulting in degradation during production, purification, or storage. Niemer and colleagues demonstrated that *N. benthamiana* tissues exhibit antibody-degrading activities, as evidenced by the degradation of CHO-derived 2F5 monoclonal antibody when treated with total soluble leaf extract and intercellular fluid from *N. benthamiana* [41]. Alternatively, glycoengineering strategies in plants can enhance the efficacy of the Fc-containing proteins. For instance, *N. benthamiana* was engineered to produce a CD27-targeted antibody (Varlilumab) with terminal galactose residues through co-expression of murine β1,4-galactosyltransferase and *Arabidopsis thaliana* β1,3-galactosyltransferase [42]. This galactosylation modification enhances the stability of CH2 domain in the Fc region and improves therapeutic efficacy by increasing ADCC and CDC activities, as demonstrated by Nguyen et al. [43]. Additionally, glycoengineered plants that downregulate the expression of plant-specific glycans offer a promising approach to reduce the immunogenicity of plant-produced recombinant glycoproteins [44].

Recombinant hIL-15 has been produced in various expression systems, including bacterial systems like *E. coli* and yeast expression platforms [45,46]. There are no prior reports of hIL-15-Fc production in a plant expression system. Meanwhile, similar studies have reported the production of Fc-hIL-2 fusion protein in *N. benthamiana* [47] and hIL-15-Fc in HEK-239 and CHO-K1 cells. In this study, we focused on optimizing the expression of hIL-15-Fc in *N. benthamiana* and characterized the plant-derived protein. We further assessed its biological activity in HaCaT cells. Optimization included the evaluation of different gene cassettes, tobacco plant age, agroinfiltration cell density, and post-infiltration harvest time.

The variation in expression levels between different constructs may be attributed to factors such as codon optimization, subcellular targeting, and the inclusion of endoplasmic reticulum (ER) retention sequence SEKDEL. Previous research suggests that codon optimization can impact protein expression by making the codon usage more favorable for the host organism [48]. For example, a proteomic analysis revealed significant expression increases, ranging from 4.9- to 7.1-fold for human clotting factor VIII and from 22.5- to 28.1-fold for polio viral capsid protein 1 when codon-optimized genes were utilized [49]. Codon optimization involves modifying the DNA sequence to match the host's codon usage preferences, including the replacement of rare codons with those favored by the expression host [50]. This strategy enhances translation efficiency and protein expression levels and was applied in the present study. On one hand, signal peptides facilitate efficient targeting of recombinant proteins to the secretory pathway, directing them to compartments where they are less likely to be degraded, thus increasing protein accumulation [51]. Additionally, the ER retention sequence SEKDEL has been shown to further enhance protein expression and stability in plants [52,53]. Our study indicated that the construct "SP-hIL-15-Fc-KD", which includes both an N-terminal signal peptide and a C-terminal ER retention sequence, achieved the highest expression level of hIL-15-Fc compared to the other constructs. Expression levels of "SP-hIL-15-Fc-KD" were 2.9-fold higher than those of "SP-hIl-15-Fc", which contained only the signal peptide at the N-terminus. However, no detectable signal was observed for the "hIL-15-Fc" construct, preventing a direct comparison of the impact of leader and retention sequences. These findings suggest that the ER retention peptide enhances protein expression, consistent with previous research [52].

One of the factors that could affect the protein expression is the age of plants. Our study indicated that 3-week-old *N. benthamiana* expressed the maximum level of hIL-15-Fc compared to the older plants. Previous research has similarly shown that younger tomato plants have higher protein content likely due to reduced cell aging and senescence-related effects [54]. Concentrations of *Agrobacterium* also influenced the amount of protein that we can detect. Higher OD_{600} values could lead to overgrowth and result in excessive damage to plant tissue and, subsequently, reduced protein yields [55]. Meanwhile, a low OD_{600} concentration resulted in a lower vector transfer efficiency, leading to suboptimal protein expression levels. Harvest timing post-infiltration was another key variable, with optimal hIL-15-Fc expression observed at 4 dpi, while levels declined at 8 and 10 dpi. The expression decreased with longer incubation periods, potentially due to protein degradation, physiological changes in the plant post-infiltration, silencing mechanisms against foreign genes, and limited duration of transient expression by *Agrobacterium* [55,56]. Previous literature suggested that the incubation period following infiltration affects the expression of other recombinant proteins, including human epidermal growth factor and human vascular endothelial growth factor in tobacco plants [57,58], with peak expression at 4–6 dpi in tobacco plants [55,57,58].

In this study, hIL-15-Fc was successfully expressed in *N. benthamiana*, achieving a yield of 33.8 μg of per gram of fresh weight. Prior research have reported hIL-15 production yields of 75 mg/L in *Pichia pastoris* [46] and 120 mg/L in *E. coli* [59], but this is the first report of hIL-15-Fc production in plant system. SDS-PAGE and Western blot analyses showed two major bands of the purified hIL-15-Fc under non-reducing conditions at approximately >100 kDa, indicating potential oligomers or aggregates formed by Fc domain oligomerization via disulfide bonds [60]. Under reducing condition, a primary band was detected at ~50 kDa, suggesting glycosylation or other post-translational modifications characteristic of plant-produced proteins. Additional bands around 100 and 150 kDa may correspond to incomplete reduction of disulfide bonds, though this has not been confirmed in this study. These SDS-PAGE and Western blot results align with the expected size range for hIL-15-Fc, which exceeds the typical hIL-15 protein size of 14–15 kDa due to the added Fc domain (25 kDa) [61–63]. Based on the molecular weight estimates of hIL-15 and Fc tag, the fusion protein was anticipated at be around 40 kDa as a monomer and approximately 80 kDa in dimeric form. However, observed molecular weights were slightly higher, potentially due to glycosylation of both hIL-15 and Fc regions, which can increase overall protein mass with glycan attachment [64]. Peptide mapping further confirmed the primary structure of our plant-produced hIL-15-Fc. This approach has been widely utilized in earlier studies for sequence validation of recombinant hIL-15 expressed in *E. coli* [65].

The bioactivity assessment of hIL-15-Fc was performed using HaCaT cells. Previous studies have shown that IL-15 can promote HaCaT cell proliferation and migration, contributing to wound healing. Treatment of HaCaT cells with concentrations of 1, 10, or 100 ng/ml can enhance cell proliferation through 72 h period. Moreover, treatment with 100 ng/ml of rhIL-15 significantly improved HaCaT cell migration compared to the untreated control cells [4]. Even though our hIL-15 was fused with Fc, we can observe similar effects in terms of HaCaT cell proliferation and migration. The mechanisms behind IL-15-induced cell proliferation and anti-apoptotic effects on HaCaT cells involves the activation of ERK 1/2 and AKT phosphorylation pathways [5]. However, there have been no reports on the biological activities of plant-based hIL-15-Fc in HaCaT cells. Notably, hIL-15 is well-established for its role in regulating various immune cells, such as promoting T cell activation and proliferation, stimulating NK cells, and enhancing B cell function [66,67]. The bioactivity of plant-produced hIL-15-Fc in immune cells should be further evaluated to assess its therapeutic potential.

5. Conclusion

In conclusion, we successfully optimized the expression of hIL-15-Fc in *N. benthamiana* and confirmed the characteristics and functional activity of the fusion protein. The plant-produced hIL-15-Fc stimulated both the proliferation and migration of human keratinocytes *in vitro*.

These findings highlight the potential of plant-based expression systems as a viable alternative to traditional platforms for producing functional hIL-15. Future studies should investigate the biological activity of plant-produced hIL-15-Fc in immune cells and evaluate its therapeutic potential through *in vivo* studies.

CRediT authorship contribution statement

Chalatorn Charnsatabut: Writing – review & editing, Writing – original draft, Methodology, Conceptualization. **Pipob Suwanchaikasem:** Writing – original draft, Methodology. **Kaewta Rattanapisit:** Methodology, Investigation, Formal analysis. **Iksen Iksen:** Writing – original draft, Methodology. **Varisa Pongrakhananon:** Writing – review & editing, Investigation. **Christine Joy I. Bulaon:** Writing – review & editing, Writing – original draft, Methodology. **Waranyoo Phoolcharoen:** Writing – review & editing, Investigation, Funding acquisition, Conceptualization.

Declaration of competing interest

Waranyoo Phoolcharoen is a founder/shareholder of Baiya Phytopharm Co., Ltd. Thailand. Authors Pipob Suwanchaikasem, Kaewta Rattanapisit, and Christine Joy I. Bulaon are employed by Baiya Phytopharm Co., Ltd. The remaining authors declare no conflicts of interest.

Acknowledgement

The authors express their gratitude to Prof. Supaart Sirikantaramas, Ph.D. for providing the *N. benthamiana* seeds.

Funding

The author (Chalatorn Charnsatabut) is financially supported by Chulalongkorn University Graduate Scholarship to commemorate the 72nd Anniversary of His Majesty King Bhumibol Adulyadej. This research has received funding support from the NSRF via the Program Management Unit for Human Resources & Institutional Development, Research and Innovation (PMU-B) [grant number B13F660137]; the 90th Anniversary of Chulalongkorn University Fund (Ratchadaphisek Somphot Endowment Fund) from Chulalongkorn University; and National Research Council of Thailand (NRCT) and Chulalongkorn University [grant number N42A670577].

Supplementary materials

Supplementary material associated with this article can be found, in the online version, at doi:10.1016/j.btre.2025.e00889.

Data availability

Data will be made available on request.

References

[1] K.H. Grabstein, et al., Cloning of a T cell growth factor that interacts with the β chain of the interleukin-2 receptor, Science (1979) 264 (5161) (1994) 965–968.
[2] T.A. Waldmann, Y. Tagaya, The multifaceted regulation of interleukin-15 expression and the role of this cytokine in NK cell differentiation and host response to intracellular pathogens, Annu. Rev. Immunol. 17 (1999) 19–49.
[3] X. Tan, L. Lefrançois, Novel IL-15 isoforms generated by alternative splicing are expressed in the intestinal epithelium, Genes & Immunity 7 (5) (2006) 407–416.
[4] A.M. Jones, et al., The clinical significance and impact of interleukin 15 on keratinocyte cell growth and migration, Int. J. Mol. Med. 38 (3) (2016) 679–686.
[5] S. Yano, et al., Interleukin 15 induces the signals of epidermal proliferation through ERK and PI 3-kinase in a human epidermal keratinocyte cell line, HaCaT. Biochemical and Biophysical Research Communications 301 (4) (2003) 841–847.
[6] A. Ward, et al., *E. coli* expression and purification of human and cynomolgus IL-15, Protein Expr. Purif. 68 (1) (2009) 42–48.
[7] K.-p. Han, et al., IL-15:IL-15 receptor alpha superagonist complex: high-level co-expression in recombinant mammalian cells, purification and characterization, Cytokine 56 (3) (2011) 804–810.
[8] W. Sun, et al., High level expression and purification of active recombinant human interleukin-15 in Pichia pastoris, J. Immunol. Methods 428 (2016) 50–57.
[9] Phase I study of recombinant interleukin 15 in combination with checkpoint inhibitors Nivolumab and Ipilimumab in subjects with refractory cancers. 2017.
[10] C. Tan, T.A. Waldmann, Bench-to-bedside translation of interleukin-15 for immunotherapy: principles and challenges, Expert. Opin. Drug Deliv. 17 (7) (2020) 895–898.
[11] M.J.B. Burnett, A.C. Burnett, Therapeutic recombinant protein production in plants: challenges and opportunities, Plants. People Planet. 2 (2) (2020) 121–132.
[12] M.M. Goodin, et al., Nicotiana benthamiana: its history and future as a model for plant–Pathogen interactions, Molecular Plant-Microbe Interactions®, 21 (8) (2008) 1015–1026.
[13] J. Bally, et al., The rise and rise of Nicotiana benthamiana : a plant for all reasons, Annu Rev. Phytopathol. 56 (2018) 405–426.
[14] S. Knapp, M.W. Chase, J.J. Clarkson, Nomenclatural changes and a new sectional classification in Nicotiana (Solanaceae), Taxon. 53 (1) (2004) 73–82.
[15] K. Moustafa, A. Makhzoum, J. Trémouillaux-Guiller, Molecular farming on rescue of pharma industry for next generations, Crit. Rev. Biotechnol. 36 (5) (2016) 840–850.
[16] B. Shanmugaraj, C.J.I. Bulaon, W. Phoolcharoen, Plant Molecular farming: a viable platform for recombinant biopharmaceutical production, Plants 9 (2020), https://doi.org/10.3390/plants9070842.
[17] S. Wylie, H. Li, Historical and scientific evidence for the origin and cultural importance to Australia's First-Nations peoples of the laboratory accession of Nicotiana benthamiana, a model for plant virology, Viruses. 14 (4) (2022).
[18] K. Vollheyde, et al., An improved Nicotiana benthamiana bioproduction chassis provides novel insights into nicotine biosynthesis, bioRxiv. (2023), p. 2023.03.06.531326.
[19] C. Huang, Receptor-fc fusion therapeutics, traps, and MIMETIBODY™ technology, Curr. Opin. Biotechnol. 20 (6) (2009) 692–699.
[20] H.K. Yu, et al., Immunoglobulin Fc domain fusion to apolipoprotein(a) kringle V significantly prolongs plasma half-life without affecting its anti-angiogenic activity, Protein Eng Des Sel, 26 (6) (2013) 425–432.
[21] H. Wang, J.S. Davis, X. Wu, Immunoglobulin Fc domain fusion to TRAIL significantly prolongs its plasma half-life and enhances its antitumor activity, Mol. Cancer Ther. 13 (3) (2014) 643–650.
[22] M.J. Knauf, et al., Relationship of effective molecular size to systemic clearance in rats of recombinant interleukin-2 chemically modified with water-soluble polymers, J. Biol. Chem. 263 (29) (1988) 15064–15070.
[23] D.M. Czajkowsky, et al., Fc-fusion proteins: new developments and future perspectives, EMBo Mol. Med. 4 (10) (2012) 1015–1028.
[24] S. Soleimanpour, et al., Fcγ1 fragment of IgG1 as a powerful affinity tag in recombinant fc-fusion proteins: immunological, biochemical and therapeutic properties, Crit. Rev. Biotechnol. 37 (3) (2017) 371–392.
[25] L.W. Moreland, et al., Treatment of rheumatoid arthritis with a recombinant human tumor necrosis factor receptor (p75)-Fc fusion protein, N. Engl. J. Med. 337 (3) (1997) 141–147.
[26] J. Tuettenberg, et al., Pharmacokinetics, pharmacodynamics, safety and tolerability of APG101, a CD95-Fc fusion protein, in healthy volunteers and two glioma patients, Int. Immunopharmacol. 13 (1) (2012) 93–100.
[27] S.D. Gillies, et al., Biological activity and *in vivo* clearance of antitumor antibody/cytokine fusion proteins, Bioconjug. Chem. 4 (3) (1993) 230–235.
[28] J.L. Flynn, et al., Major histocompatibility complex class I-restricted T cells are required for resistance to mycobacterium tuberculosis infection, Proc. Natl. Acad. Sci. u S. a 89 (24) (1992) 12013–12017.
[29] P.J. Carter, Introduction to current and future protein therapeutics: a protein engineering perspective, Exp. Cell Res. 317 (9) (2011) 1261–1269.
[30] Q. Chen, et al., Geminiviral vectors based on bean yellow dwarf virus for production of vaccine antigens and monoclonal antibodies in plants, Hum. Vaccin. 7 (3) (2011) 331–338.
[31] C. The UniProt, UniProt: the Universal Protein knowledgebase in 2023, Nucleic. Acids. Res. 51 (D1) (2023) D523–D531.
[32] M. Tschofen, et al., Plant molecular farming: much more than medicines, Annu Rev. Anal. Chem. (Palo Alto Calif) 9 (1) (2016) 271–294.
[33] R. Menassa, A. Jevnikar, J. Brandle, et al., The production of recombinant cytokines in plants, in: L. Erickson, et al. (Eds.), Molecular Farming of Plants and Animals for Human and Veterinary Medicine, Springer Netherlands: Dordrecht, 2002, pp. 319–338. Editors.
[34] A. Sirko, et al., Recombinant cytokines from plants, Int. J. Mol. Sci. 12 (6) (2011) 3536–3552.
[35] N.B. da Cunha, et al., Molecular farming of human cytokines and blood products from plants: challenges in biosynthesis and detection of plant-produced recombinant proteins, Biotechnol. J. 9 (1) (2014) 39–50.
[36] I. Kolotilin, Plant-produced recombinant cytokines IL-37b and IL-38 modulate inflammatory response from stimulated human PBMCs, Sci. Rep. 12 (1) (2022) 19450.
[37] M.T. McManus, et al., Identification of a monoclonal antibody to abscission tissue that recognises xylose/fucose-containing N-linked oligosaccharides from higher plants, Planta 175 (4) (1988) 506–512.
[38] I.B.H. Wilson, et al., Core α1,3-fucose is a key part of the epitope recognized by antibodies reacting against plant N-linked oligosaccharides and is present in a wide variety of plant extracts, Glycobiology 8 (7) (1998) 651–661.

[39] B. Arsova, M. Watt, B. Usadel, Monitoring of plant protein post-translational modifications using targeted proteomics, Front. Plant Sci. (2018) 9.
[40] V. Muleya, et al., (De)Activation (Ir)reversibly or degradation: dynamics of post-translational protein modifications in plants, Life 12 (2022), https://doi.org/10.3390/life12020324.
[41] M. Niemer, et al., The human anti-HIV antibodies 2F5, 2G12, and PG9 differ in their susceptibility to proteolytic degradation: down-regulation of endogenous serine and cysteine proteinase activities could improve antibody production in plant-based expression platforms, Biotechnol. J. 9 (4) (2014) 493–500.
[42] K.D. Nguyen, et al., Production and N-glycan engineering of Varlilumab in Nicotiana benthamiana, Front. Plant Sci. 14 (2023) 1215580.
[43] M. Kiyoshi, et al., Assessing the heterogeneity of the fc-glycan of a therapeutic antibody using an engineered fcγreceptor IIIa-immobilized column, Sci. Rep. 8 (1) (2018) 3955.
[44] L. Montero-Morales, H. Steinkellner, Advanced plant-based glycan engineering, Front. Bioeng. Biotechnol. 6 (2018) 81.
[45] V.V. Vyas, et al., Clinical manufacturing of recombinant human interleukin 15. I. Production cell line development and protein expression in *E. coli* with stop codon optimization, Biotechnol. Prog. 28 (2) (2012) 497–507.
[46] W. Sun, et al., High level expression and purification of active recombinant human interleukin-15 in Pichia pastoris, J. Immunol. Methods 428 (2016) 50–57.
[47] C. Marusic, et al., Production of an active anti-CD20-hIL-2 immunocytokine in icotiana benthamiana, Plant Biotechnol. J. 14 (1) (2016) 240–251.
[48] Y. Wakasa, F. Takaiwa, The use of rice seeds to produce human pharmaceuticals for oral therapy, Biotechnol. J. 8 (10) (2013) 1133–1143.
[49] K.C. Kwon, et al., Codon optimization to enhance expression yields insights into chloroplast translation, Plant Physiol. 172 (1) (2016) 62–77.
[50] H. Fu, et al., Codon optimization with deep learning to enhance protein expression, Sci. Rep. 10 (1) (2020) 17617.
[51] S.M. Rozov, E.V. Deineko, Increasing the efficiency of the accumulation of recombinant proteins in plant cells: the role of transport signal peptides, Plants. (Basel) (19) (2022) 11.
[52] A. Schouten, et al., The C-terminal KDEL sequence increases the expression level of a single-chain antibody designed to be targeted to both the cytosol and the secretory pathway in transgenic tobacco, Plant Mol. Biol. 30 (4) (1996) 781–793.
[53] S. Petruccelli, et al., A KDEL-tagged monoclonal antibody is efficiently retained in the endoplasmic reticulum in leaves, but is both partially secreted and sorted to protein storage vacuoles in seeds, Plant Biotechnol. J. 4 (5) (2006) 511–527.
[54] Y. Yu, et al., The role of plant age and leaf position on protein extraction and phenolic compounds removal from tomato (Solanum lycopersicum) leaves using food-grade solvents, Food Chem. 406 (2023) 135072.
[55] K. Norkunas, et al., Improving agroinfiltration-based transient gene expression in Nicotiana benthamiana, Plant Methods 14 (1) (2018) 71.
[56] M.J. Stephenson, et al., Transient expression in Nicotiana Benthamiana leaves for triterpene production at a preparative scale, J. Vis. Exp. (138) (2018).
[57] C.J.I. Bulaon, et al., Rapid transient expression of functional human vascular endothelial growth factor in Nicotiana benthamiana and characterization of its biological activity, Biotechnol. Rep. (Amst) 27 (2020) e00514.
[58] O. Hanittinan, et al., Expression optimization, purification and *in vitro* characterization of human epidermal growth factor produced in Nicotiana benthamiana, Biotechnol. Rep. (Amst) 28 (2020) e00524.
[59] N. Ahmed, et al., Method for efficient soluble expression and purification of recombinant human interleukin-15, Protein Expr. Purif. 177 (2021) 105746.
[60] G.M. Edelman, et al., The covalent structure of an entire gammaG immunoglobulin molecule, Proc. Natl. Acad. Sci. u S. a 63 (1) (1969) 78–85.
[61] S. Zhang, et al., Biological effects of IL-15 on immune cells and its potential for the treatment of cancer, Int. Immunopharmacol. (2021) 91.
[62] T.A. Waldmann, The biology of interleukin-2 and interleukin-15: implications for cancer therapy and vaccine design, Nature Reviews Immunology 6 (8) (2006) 595–601.
[63] M.C. Sneller, et al., IL-15 administered by continuous infusion to rhesus macaques induces massive expansion of CD8+ T effector memory population in peripheral blood, Blood 118 (26) (2011) 6845–6848.
[64] H.S. Lee, Y. Qi, W. Im, Effects of N-glycosylation on protein conformation and dynamics: protein Data Bank analysis and molecular dynamics simulation study, Sci. Rep. 5 (1) (2015) 8926.
[65] V.V. Vyas, et al., Clinical manufacturing of recombinant human interleukin 15. I. Production cell line development and protein expression in *E. coli* with stop codon optimization, Biotechnol. Prog. 28 (2) (2012) 497–507.
[66] W. Jiang, et al., hIL-15-gene modified human natural killer cells (NKL-IL15) exhibit anti-human leukemia functions, J. Cancer Res. Clin. Oncol. 144 (7) (2018) 1279–1288.
[67] S. Hazama, et al., Tumour cells engineered to secrete interleukin-15 augment anti-tumour immune responses *in vivo*, Br. J. Cancer 80 (9) (1999) 1420–1426.